

# Ethanol Electro-oxidation on Pt/C Electrocatalysts: An “In Situ” Raman Spectroelectrochemical Study

Rodrigo F. B. De Souza · Érico Teixeira Neto ·  
Marcelo L. Calegari · E. A. Santos ·  
Herculano S. Martinho · Mauro Coelho dos Santos

Published online: 12 January 2011  
© Springer 2011

**Abstract** This work presents an “in situ” spectroelectrochemical study of the ethanol oxidation reaction on Pt/C electrocatalysts prepared by the polymeric precursor method. Characterization of the electrocatalysts was performed with X-ray diffraction, Raman spectroscopy, and cyclic voltammetry measurements. The average crystallite size was estimated as 7 nm, in agreement with the value reported in the literature for these types of electrocatalysts. The cyclic voltammetry characterization in an acidic medium presented the expected voltammetric behavior for polycrystalline Pt/C. The ethanol oxidation process was successfully employed “in situ”, making use

of an optical probe for excitation and collection of the Raman scattering signal. In this configuration it was possible to track the formation of the main products—CO, CO<sub>2</sub> indirectly, acetaldehyde, and acetic acid—and to measure the decay of the ethanol concentration. The results indicate that the optical probe-based Raman spectroscopy technique is a very effective tool for studying “in situ” electrochemical oxidation reactions of ethanol. It might also be a very promising characterization technique for studies of the “in situ” electrochemical oxidation of small organic molecules.

**Keywords** Ethanol oxidation reaction · Electrocatalysis · Pt nanoparticles · “In situ” Raman spectroscopy · Polymeric precursor method · Pt/C

R. F. B. De Souza · É. T. Neto · M. C. dos Santos (✉)  
LEMN—Laboratório de Eletroquímica e Materiais  
Nanoestruturados—CCNH—Centro de Ciências Naturais e  
Humanas, UFABC—Universidade Federal do ABC,  
Rua Santa Adélia 166, Bairro Bangu,  
09.210-170, Santo André, São Paulo, Brazil  
e-mail: mauro.santos@ufabc.edu.br

H. S. Martinho  
GMAV—Grupo de Materiais e Métodos Avançados—CCNH—  
Centro de Ciências Naturais e Humanas, UFABC—Universidade  
Federal do ABC,  
Rua Santa Adélia 166, Bairro Bangu,  
09.210-170, Santo André, São Paulo, Brazil

M. L. Calegari  
Grupo de Materiais Eletroquímicos e Métodos Eletroanalíticos—  
Instituto de Química de São Carlos, Universidade de São Paulo,  
Caixa Postal 780, 13566-590, São Carlos, São Paulo, Brazil

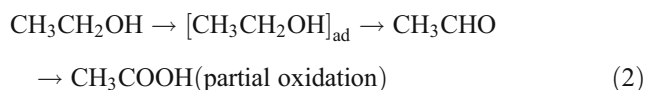
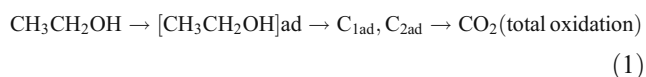
E. A. Santos  
IP&D—Universidade do Vale do Paraíba,  
Avenida Shishima Hifumi, 2911, Urbanova,  
São José dos Campos, São Paulo, Brazil

## Introduction

Currently, ethanol electrooxidation on Pt-based electrocatalysts is one of the most intensively studied subjects in surface (interfacial) electrochemistry [1–5]. Ethanol is safer, can be produced in great quantities from biomass [6], and, when compared with methanol, has a higher energy density (8.01 vs 6.09 kWhkg<sup>-1</sup>) [7]. Thus, ethanol is considered to be a more attractive fuel for direct alcohol fuel cells.

The main challenge for the wide development of direct ethanol fuel cells and new catalytic materials technologies is the lack of detailed knowledge concerning the reaction mechanism. Currently, in spite of the lack of conclusive information concerning the ethanol oxidation process, it is well accepted that in acidic solutions the reaction proceeds

through a series of parallel reactions, summarized in the following scheme [8]:



The complete electro-oxidation of ethanol to  $\text{CO}_2$  involves the cleavage of the C–C bond, which requires rather high activation energy. In this process two adsorbed intermediates,  $\text{C}_{1\text{ad}}$  and  $\text{C}_{2\text{ad}}$ , with one and two carbons, respectively, are formed. Small  $\text{C}_1$  and  $\text{C}_2$  intermediates are of special interest due to their direct oxidation in energy-conversion designs, such as fuel cell devices [9, 10]. Therefore, their identification in methanol, ethanol, and formic acid on platinum-group metals had been widely investigated [11, 12].

Unfortunately, it is impossible to discuss the detailed mechanism of electro-oxidation based only on cyclic voltammetry and chronoamperometry. The superficially adsorbed intermediate species of organic molecular oxidation processes have usually been identified by surface analytical techniques such as “in situ” IR spectroscopy [10–13], sum frequency generation [14], differential electrochemical mass spectrometry [15–17], ellipsometry [18], and others. The main limitation of these techniques lies in the high quality requirements of the surface in order to get reliable spectral data. Usually, smooth or single crystalline electrodes are able to fulfill these requirements; however, there are many papers that used carbon supported nanoparticles [19–22] using a gold disc as substrate for working electrodes, because both its reflective properties and its good quality spectra. Thus, the development of more versatile experimental probes to monitor the electrochemical process in highly roughened electrode surfaces without reflective supports as, for example, gold disc is of obvious interest.

In this way, the inelastic scattering of light by Raman spectroscopy could be assigned as a useful probe to obtain spectral information on diverse surface bonding, revealing details about the nature of the surface interaction, coverage, and co-adsorption. This is of great practical importance when applied to surface catalytic processes, such as  $\text{C}_1$  and  $\text{C}_2$  oxidation, especially under vigorous reaction conditions [11]. One example of the potential of this technique is the pioneering work of Ren et al. [23], which studied methanol oxidation in an aqueous sulfuric acid solution as a function of the surface roughness of platinum. Surface-enhanced Raman spectroscopy has also been performed [9, 11, 24–29] on some rough transition metal electrodes to detect species produced during electrochemical redox processes [24–31].

However, to the best of our knowledge, all “in situ” Raman studies presented in the literature were restricted to the methanol case. Thus, this work concerns the “in situ” monitoring of the ethanol oxidation with electrocatalysts containing a very low Pt load on carbon by Raman spectroscopy.

## Experimental

### Preparation of Electrocatalysts

Pt/C (20% w/w on black carbon) electrocatalyst were prepared using the polymeric precursor method as described by De Souza et al. [32–34], and the mass ratio was 1:50:400 (metallic precursor/citric acid (CA)/ethylene glycol (EG)). The catalysts were prepared by placing a predetermined volume of each resin into an appropriate amount of carbon vulcan XC-72R (Cabot Corporation), followed by the addition of enough EG to cover the carbon powder. These mixtures were homogenized in an ultrasonic bath for over 60 min and then thermally treated at 400 °C for 2 h in a  $\text{N}_2$  atmosphere.

### Physical Characterization

The crystalline structures of the investigated catalysts were determined by using the powder X-ray diffraction (XRD) technique. The data were recorded with a Rigaku diffractometer (Miniflex model), using Cu KR radiation source (1.5406 Å, 30 kV, and 15 mA). Approximately, 30 mg of the powdered samples was placed in a glass sample holder and compressed with a glass slide to obtain a uniform distribution. The  $2\theta$  Bragg angles were scanned over a range of 30–70° at a rate of 2°/min with a 0.02° angular resolution.

### Electrochemical Measurements

Electrochemical measurements were performed at room temperature using an Autolab PGSTAT 302N potentiostat. Glassy carbon (GC) electrodes were employed as support for the working ones (0.166 cm<sup>2</sup> of geometric area). In a three-compartment electrochemical cell, a large Pt ring was used as a counter electrode. All potentials were referred to a reversible hydrogen electrode. Before each experiment, the GC support was polished with alumina suspension (1 μm) to a mirror finish and washed in a mixture of ethanol and water. We used Milli-Q water (Millipore®) in all experimental procedures.

The working electrodes were constructed by dispersing 10 mg of electrocatalyst powder in 1 ml water and mixing for 5 min in an ultrasonic bath. Soon afterwards, 20 μl of

5% Nafion® solution was added to the suspension, and it was mixed again in an ultrasonic bath for 15 min. Aliquots of 16  $\mu\text{L}$  of the dispersion fluid were pipetted onto the GC surface. Finally, the electrode was dried at 60 °C for 20 min and hydrated for 5 min in water.

The cyclic voltammetric and chronoamperometric experiments were performed in solutions of (1) 0.5 molL<sup>-1</sup> HClO<sub>4</sub> and (2) 0.5 molL<sup>-1</sup> HClO<sub>4</sub> plus 2 molL<sup>-1</sup> of ethanol.

#### “In Situ” Raman Spectroscopy

The “in situ” Raman setup consisted of a tunable Lithrow-configuration diode laser with  $\lambda=785$  nm (Sacher Lasertechnik) for Raman excitation, a spectrometer (PiActon SpectraPro model 2500i) equipped with a N<sub>2</sub>-cooled CCD detector (Princeton Instruments Spec-10) and an optical probe (EMVISION LLC) for both exciting and collecting the signal. Attached to the spectrometer end of the optical probe, there was a set of notch filters for stray-light removal. All measurements were made in the backscattering configuration. The laser power was fixed to 40 mW on the sample, and the typical acquisition time was 60 s.

#### Experimental Arrangement

The experimental apparatus for the Raman measurements were taken making use of a commercial optical fiber probe (EMVISION LLC). This optical probe is composed of a set of seven 600  $\mu\text{m}$  diameter optical fibers arranged as shown on Fig. 1a below. In this setup the central fiber deliver the laser light to the sample and the other six collect the scattered light. Thus the laser spot had 600  $\mu\text{m}$  of diameter. The best signal to noise ratio was found positioning the fiber 3 mm above the electrode. The solution layer was nearly 2 mm above the electrode as shown in Fig. 1b.

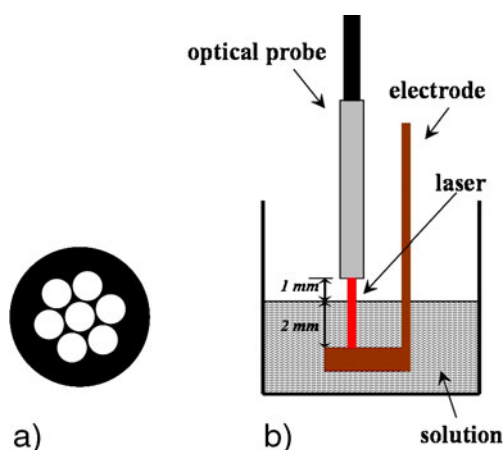


**Fig. 1** a Optical fiber with emissary and collectors. b Electrochemical cell with the optical probe

## Results and Discussion

### Characterization of Pt/C Electrocatalysts

The XRD peak pattern analysis was carried out to estimate the mean crystallite sizes and also for the structural characterization of the Pt/C electrocatalysts. It is well known that it is possible to estimate the average particle size from XRD data, which are in good agreement with transmission electron microscopy data (less than 6% deviation) [35].

Figure 2a shows the XRD diffractogram of the Pt/C electrocatalysts prepared using the precursor solution 1/50/400 (Pt/CA/EG) mass ratio and thermally treated at 400 °C.

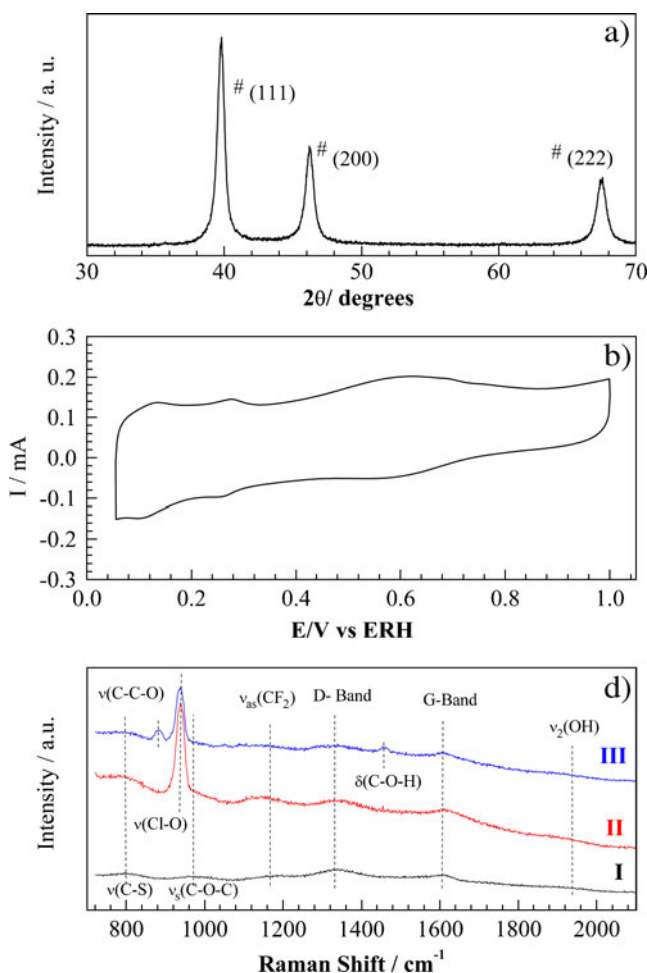


**Fig. 2** a XRD diffractogram of the Pt/C electrocatalysts. The characteristic (111), (200), and (220) Pt Bragg peaks were observed at  $2\theta=39.800^\circ$ ,  $46.200^\circ$ , and  $67.460^\circ$ , respectively. b Voltammetric profile for the Pt/C electrocatalyst in acidic medium: HClO<sub>4</sub> aqueous solution (0.5 molL<sup>-1</sup>), scan rate=10 mVs<sup>-1</sup>. c “In situ” Raman spectra of the Pt/C electrocatalyst immobilized with Nafion® suspension at the glass carbon electrode, under three conditions: in air (curve I), in HClO<sub>4</sub> aqueous solution (0.5 molL<sup>-1</sup>) (curve II), and in an aqueous solution of HClO<sub>4</sub> (0.5 molL<sup>-1</sup>) plus 1 molL<sup>-1</sup> of ethanol (curve III). Characteristic vibrational bands are also shown

The characteristic (111), (200), and (220) Pt Bragg peaks were observed at  $2\theta=39.800^\circ$ ,  $46.200^\circ$ , and  $67.460^\circ$ , respectively, in good agreement with the Pt standard (JCPDS PDF#04-0802). The average crystallite size was estimated applying the Debye–Scherrer equation [36] to the (111) reflection. The value obtained was 7 nm, in agreement with that reported on literature for this kind of electrocatalyst [37, 38].

The typical voltammetric profile for the Pt/C electrocatalyst in an acidic medium is presented in Fig. 2b. The fairly resolved Pt features (hydrogen adsorption/desorption and formation and reduction of PtO) are in accordance with those discussed in the literature [32, 38, 39].

Figure 2c shows the “in situ” Raman spectra of the Pt/C electrocatalyst immobilized with Nafion® suspension at the GC electrode, under three conditions: (1) in air (spectrum I), (2) in HClO<sub>4</sub> aqueous solution (0.5 molL<sup>-1</sup>) (spectrum II), and (3) in an aqueous solution of HClO<sub>4</sub> (0.5 molL<sup>-1</sup>) plus 2 molL<sup>-1</sup> of ethanol (spectrum III).

In spectrum I, it is possible observe the D and G bands of carbon at 1,338 and 1,593 cm<sup>-1</sup> [38, 40, 41], respectively. Additionally, bands at 794, 974, and 1,166 cm<sup>-1</sup> could be assigned to  $\nu$  (C–S),  $\nu_s$  (C–O–C), and  $\nu$  (CF<sub>2</sub>) of Nafion® [42]. The flat band at 1,938 cm<sup>-1</sup> corresponds to  $\nu_2$  (OH) [42].

Spectrum II presented only one new band at 934 cm<sup>-1</sup>, which corresponds to  $\nu$  (Cl–O<sub>4</sub>) of HClO<sub>4</sub> [43].

In addition to the above-cited vibrational bands, spectrum III presented two characteristic bands of ethanol at 882 and 1,456 cm<sup>-1</sup> ( $\nu_s$  (C–C–O) [44, 45] and  $\delta$  (C–O–H) [42, 45], respectively) and three remaining tiny bands at 1,051, 1,095, and 1,276 cm<sup>-1</sup>, associated with  $\nu_a$  (C–C–O) [45],  $\gamma$  (C–O–H) [44, 45], and  $t$  (CH<sub>2</sub>)+ $\delta$  (C–O–H) [44–46], respectively.

#### Electrochemical Profiles for Ethanol Oxidation on Pt/C Electrocatalysts

Figure 3 presents the cyclic voltammetry and chronoamperometry (inset) results for the ethanol oxidation reaction on Pt/C electrocatalysts in an acidic medium. To the best of our knowledge, this is the first reported profile concerning the precursor polymeric method to obtain only Pt/C as an electrocatalyst. The observed feature is in agreement with those reported by several papers [4, 17, 47]. The observed onset potential for the ethanol oxidation was close to 0.35 V, which is lower than that found in the literature (0.38 V) [17]. Furthermore, it is important to stress that the chronoamperometric curve presents a high current density of 5.2 mA mg<sub>Pt</sub><sup>-1</sup> compared with that observed in the literature for the same process [17]. We can understand these findings by recalling that we are working with higher ethanol concentrations.

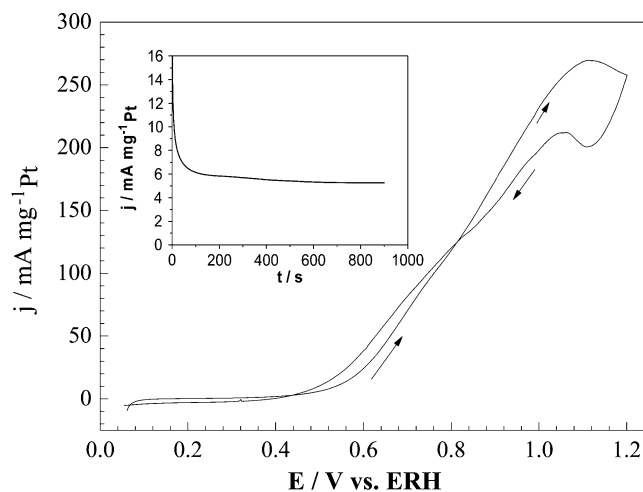


**Fig. 3** Cyclic voltammetry and chronoamperometry (inset, oxidation potential=0.5 V vs. RHE, time=900 s) results for the ethanol oxidation reaction on Pt/C electrocatalysts in an acidic medium (aqueous solution of HClO<sub>4</sub> (0.5 molL<sup>-1</sup>) plus 1 molL<sup>-1</sup> of ethanol)

#### “In Situ” Raman Results

The Raman spectra obtained along the ethanol oxidation process are shown in Fig. 4. At zero voltage, almost all bands presented well defined and intense shapes. By increasing the potential, the intensity and linewidth of several peaks were modified. In order to associate these changes with increasing or decreasing concentrations of specific species produced during the ethanol oxidation, all bands were deconvoluted to Lorentzian lineforms. Thus, the intensity and linewidth of each band were individually analyzed. In this work, we will focus on only the intensity variations (Fig. 5). Unfortunately, some weak vibrational

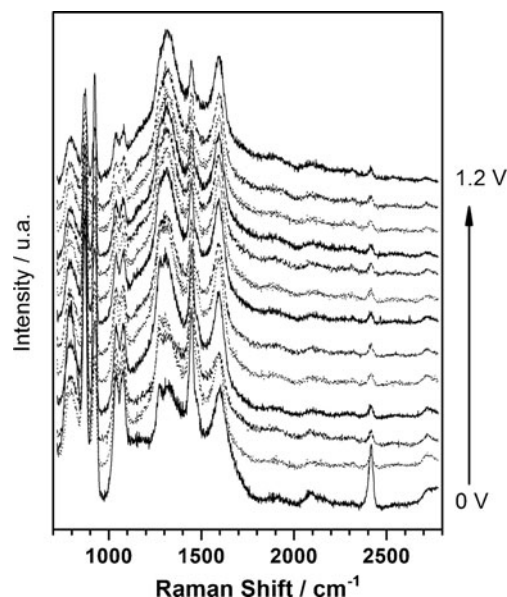
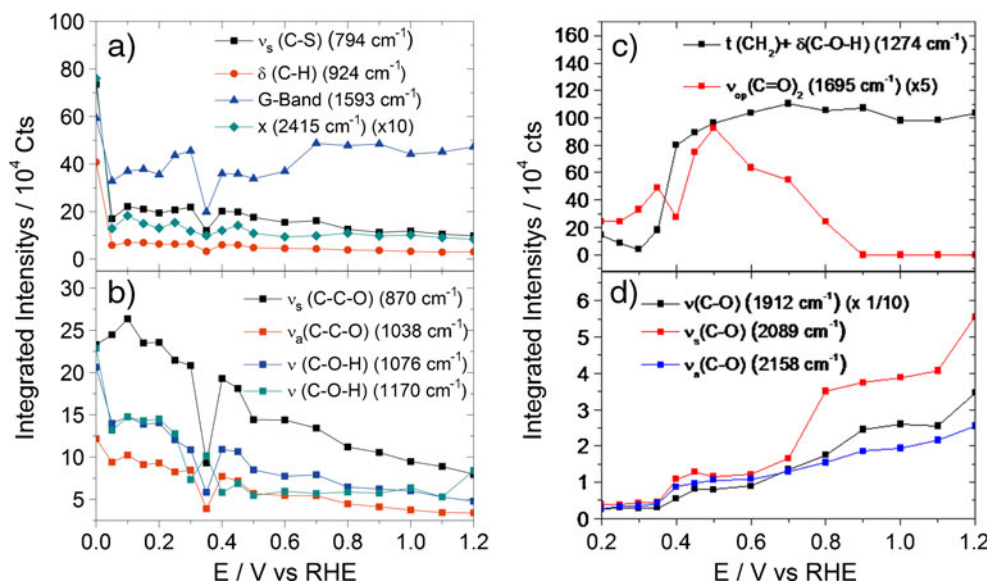


**Fig. 4** “In situ” Raman spectra obtained during the ethanol oxidation process for each 100 mV

**Fig. 5** Voltage dependence of the vibrational band intensities, acquired for deconvoluted to Lorentzian lineforms of all bands shown in Fig. 4. (More details in text.)



bands were superimposed with other ones, smearing out their voltage dependence. In particular, this occurred with the D band ( $1,338\text{ cm}^{-1}$ ) and  $\delta$  (C–O–H) ( $1,453\text{ cm}^{-1}$ ).

Figure 5a shows the voltage dependence of the  $\nu$  (C–S),  $\gamma$  (C–H), and G band intensities. The band at  $2,415\text{ cm}^{-1}$  remained unidentified. A commonly observed feature was the sudden and strong intensity decrease ( $\sim 1/3$ ) when setting 50 mV voltage. Recalling that all these bands are related to electrode compositional elements (Nafion and carbon), this decrease could originate from the adsorption of intermediate species on the electrode. At 0.35 V, a transient intensity decrease was observed in all bands. This point coincides with the onset of the oxidation process. For higher voltages, all bands, except the G band, show a smooth decreasing behavior. The G band intensity behavior needs to be considered with relative care due to the presence of a shoulder at  $1,587\text{ cm}^{-1}$ . This shoulder is probably due to (C=C) vibration [45], which could be related to intermediates of ethanol oxidation. Above 0.35 V, this shoulder collapses into the G-band position, and the reported intensity behavior is a superposition of these two species. An almost constant G-band intensity is expected. Otherwise, the  $1,587\text{ cm}^{-1}$  shoulder intensity could vary in a complex way.

Figure 5b shows the behavior of four ethanol bands:  $\nu_s$  (C–C–O),  $\nu_a$  (C–C–O),  $\nu$  (C–O–H), and  $\gamma$  (C–O–H). A transient intensity decrease at 0.35 V was also observed in all cases. Due to ethanol consumption, all bands displayed a consistent intensity decreasing.

Figure 5c shows the voltage dependence of the  $t$  ( $\text{CH}_2$ )+ $\delta$  (C–O–H) ( $1,274\text{ cm}^{-1}$ ) [44, 46] and  $\delta$  (C=O) ( $1,695\text{ cm}^{-1}$ ) [48] band intensities, these bands could be assigned to acetic acid and acetaldehyde respectively. Several works using FTIR in situ have also reported the formation of acetic acid and acetaldehyde in the ethanol oxidation process on

different substrates [11, 14, 22, 49–52]. Giz et al. [49] studying ethanol oxidation reaction on Pt report the appearance of acetaldehyde and acetic acid bands at 0.38 V. Regarding the band associated to acetic acid on Pt it has been observed in the literature an stabilization of the intensity near at 0.9 V [51] including experiments on Pt single crystals as substrates [11, 49, 53]. This behavior is in agreement with one here measured as can be seen in Fig. 5c. Another similarity here found with the literature [49] is that acetaldehyde band which starts decreasing at 0.75 V.

In the experiment of Fig. 5 the intensity of acetaldehyde production is lower than the one for acetic acid and  $\text{CO}_2$ . This fact is associated to the products acetic acid and  $\text{CO}_2$  requires more oxygen [49, 50, 54]. As the set up here used was in atmospheric air it can be suggested that the oxygen excess favors acetic acid and  $\text{CO}_2$  production.

$\text{CO}_2$  and CO are common and extensively measured during ethanol oxidation on Pt/C electrocatalysts [5, 14, 22, 52]. In the experiments here carried out it was possible to identify only CO. The bands for this specie was presented in Fig. 5d,  $\nu$  (C–O) ( $1,912\text{ cm}^{-1}$ ),  $\nu_s$  (C–O) ( $2,089\text{ cm}^{-1}$ ) [55], and  $\nu_{as}$  (C–O) ( $2,158\text{ cm}^{-1}$ ) [56]. Regarding the behavior associated to CO it has been found in the literature [46, 47] both an increasing beginning at 0.3 V and a decreasing after 0.6 V. This feature is similar to one in Fig. 5d. Again, considering the literature for  $\text{CO}_2$  it has been observed that there is increasing band intensity from 0.8 up to 1.0 V. After that, there is a stabilization of the band intensity [11, 22, 49, 53] following by an increasing close to 1.1 V. This is what has been found in Fig. 5d, but for CO rather than  $\text{CO}_2$ . For the reasons pointed out above, we can suggest that the increasing of CO bands intensities after 0.6 V could be associated to  $\text{CO}_2$  production from CO, since during ethanol oxidation  $\text{CO}_2$  produced depends on the breaking of C–C bond and formation of CO. As  $\text{CO}_2$

Raman active band shift (symmetric stretch) is only present at  $1,340\text{ cm}^{-1}$  and in this case is overlapped with the *d*-band of carbon at  $1,345\text{--}1,350\text{ cm}^{-1}$  and it is was not possible to measure, probably the increasing in the CO bands after 0.6 V are related to CO<sub>2</sub> production from CO at the time of the experiment. One can see CO but not CO<sub>2</sub>, than we have a possible indirect measurement of CO<sub>2</sub>.

## Conclusions

This work is the first detailed report employing an “in situ” Raman spectroelectrochemical setup for studying the ethanol oxidation process on Pt/C electrocatalysts. It was possible to trigger the formation of the main species produced during the electrochemical process, namely, CO, CO<sub>2</sub> (indirectly), acetic acid, and acetaldehyde. Furthermore, one of the two carbons intermediates was detected as well as the consumption of the ethanol. Besides, the data obtained using Raman “in situ” are complementary of the ones obtained using “in situ” FTIR reported in the literature. Other important point of this technique is the possibility of obtain spectra without use a reflective substrate, required for the FTIR “in situ” experiments. In others words, Raman spectroscopy technique “in situ” approach is very promising for the study of small organic molecule oxidation processes.

**Acknowledgements** The authors wish to thank the Brazilian Funding Institutions (CNPq 474742-32/2008-8), CAPES, and FAPESP (Processes Numbers: 05/59992-6, 301018/2006-5, 09/09145-6) and UFABC for their financial support. In addition, the authors thank Prof. Vera R.L. Constantino from IQ-USP for the use of the XRD instrument; Dr. Ângela A. Teixeira Neto for assistance with XRD analysis; and Prof. Dr. Airton A. Martin from UniVap for the use of the Raman instrumentation.

## References

1. B.C.H. Steele, A. Heinzl, *Nature* **414**, 345 (2001)
2. R. Dillon, S. Srinivasan, A.S. Aricò, V. Antonucci, *J. Power Sources* **127**, 112 (2004)
3. S. Song, P. Tsiakaras, *Appl. Catal. B* **63**, 187 (2006)
4. K.-S. Lee, I.-S. Park, Y.-H. Cho, D.-S. Jung, N. Jung, H.-Y. Park, Y.-E. Sung, *J. Catal.* **258**, 143 (2008)
5. C. Coutanceau, S. Brimaud, C. Lamy, J.M. Léger, L. Dubau, S. Rousseau, F. Vigier, *Electrochim. Acta* **53**, 6865 (2008)
6. G. Li, P.G. Pickup, *J. Power Sources* **161**, 256 (2006)
7. C. Xu, P.K. Shen, *J. Power Sources* **142**, 27 (2005)
8. E. Antolini, *J. Power Sources* **170**, 1 (2007)
9. P. Cao, Q. Zhong, Y. Sun, R. Gu, *Chem. Phys. Lett.* **376**, 806 (2003)
10. J.-T. Li, Q.-S. Chen, S.-G. Sun, *Electrochim. Acta* **52**, 5725 (2007)
11. V. Pacheco Santos, V. Del Colle, R.B. de Lima, G. Tremiliosi-Filho, *Electrochim. Acta* **52**, 2376 (2007)
12. G.A. Camara, R.B. de Lima, T. Iwasita, *J. Electroanal. Chem.* **585**, 128 (2005)
13. J. Ribeiro, D.M. dos Anjos, K.B. Kokoh, C. Coutanceau, J.M. Léger, P. Olivi, A.R. de Andrade, G. Tremiliosi-Filho, *Electrochim. Acta* **52**, 6997 (2007)
14. J.F. Gomes, B. Busson, A. Tadjeddine, G. Tremiliosi-Filho, *Electrochim. Acta* **53**, 6899 (2008)
15. J. Barranco, A.R. Pierna, *J. Power Sources* **169**, 71 (2007)
16. T. Seiler, E.R. Savinova, K.A. Friedrich, U. Stimming, *Electrochim. Acta* **49**, 3927 (2004)
17. H. Wang, Z. Jusys, R.J. Behm, *J. Power Sources* **154**, 351 (2006)
18. L. Zhou, S. Günther, D. Moszynski, R. Imbihl, *J. Catal.* **235**, 359 (2005)
19. C. Lamy, S. Rousseau, E.M. Belgsir, C. Coutanceau, J.M. Leger, *Electrochim. Acta* **49**, 3901 (2004)
20. F.C. Simões, D.M. dos Anjos, F. Vigier, J.M. Léger, F. Hahn, C. Coutanceau, E.R. Gonzalez, G. Tremiliosi-Filho, A.R. de Andrade, P. Olivi, K.B. Kokoh, *J. Power Sources* **167**, 1 (2007)
21. M. Li, A. Kowal, K. Sasaki, N. Marinkovic, D. Su, E. Korach, P. Liu, R.R. Adzic, *Electrochim. Acta* **55**, 4331 (2010)
22. J.M. Léger, S. Rousseau, C. Coutanceau, F. Hahn, C. Lamy, *Electrochim. Acta* **50**, 5118 (2005)
23. B. Ren, X.Q. Li, C.X. She, D.Y. Wu, Z.Q. Tian, *Electrochim. Acta* **46**, 193 (2000)
24. M. Bron, R. Holze, *Surf. Sci.* **457**, 178 (2000)
25. J. Solla-Gullón, R. Gómez, A. Aldaz, J.M. Pérez, *Electrochem. Commun.* **10**, 319 (2008)
26. Y.-C. Liu, K.-H. Yang, L.-H. Lin, J.-F. Tsai, *Electrochem. Commun.* **10**, 161 (2008)
27. T. Marui, S. Kajita, Y. Katayama, K. Chiba, *Electrochem. Commun.* **9**, 1331 (2007)
28. R. Mazeikiene, G. Niaura, A. Malinauskas, *Electrochim. Acta* **51**, 5761 (2006)
29. H.J. Salavagione, J. Arias-Pardilla, J.M. Pérez, J.L. Vázquez, E. Morallón, M.C. Miras, C. Barbero, *J. Electroanal. Chem.* **576**, 139 (2005)
30. K. Dokko, N. Anzue, M. Mohamedi, T. Itoh, I. Uchida, *Electrochem. Commun.* **6**, 384 (2004)
31. K. Crowley, J. Cassidy, *J. Electroanal. Chem.* **547**, 75 (2003)
32. R.F.B. De Souza, A.E.A. Flausino, D.C. Rascio, R.T.S. Oliveira, E.T. Neto, M.L. Calegario, M.C. Santos, *Appl. Catal. B* **91**, 516 (2009)
33. R.F.B. De Souza, L.S. Parreira, D.C. Rascio, J.C.M. Silva, E. Teixeira-Neto, M.L. Calegario, E.V. Spinace, A.O. Neto, M.C. Santos, *J. Power Sources* **195**, 1589 (2010)
34. A. S. Polo, M. C. Santos, R. F. B. de Souza, W. A. Alves, *J. Power Sources* **196**, 872 (2011)
35. K.J.J. Mayrhofer, J.C. Meier, S.J. Ashton, G.K.H. Wiberg, F. Kraus, M. Hanzlik, M. Arenz, *Electrochem. Commun.* **10**, 1144 (2008)
36. B.D. Cullity, *Elements of X-ray diffraction* (Addison-Wesley, Massachusetts, 1967), p. 262
37. L. Jiang, G. Sun, S. Sun, J. Liu, S. Tang, H. Li, B. Zhou, Q. Xin, *Electrochim. Acta* **50**, 5384 (2005)
38. D. Yuan, S. Tan, Y. Liu, J. Zeng, F. Hu, X. Wang, P. Shen, *Carbon* **46**, 531 (2008)
39. J.-G. Oh, C.-H. Lee, H. Kim, *Electrochem. Commun.* **9**, 2629 (2007)
40. S. Liu, C. Cai, *J. Electroanal. Chem.* **602**, 103 (2007)
41. A.E. Galetti, M.F. Gomez, L.A. Arrúa, M.C. Abello, *Appl. Catal. A* **348**, 94 (2008)
42. V. Di Noto, R. Gliubizzi, E. Negro, M. Vittadello, G. Pace, *Electrochim. Acta* **53**, 1618 (2007)
43. M. Ibrahim, M. Kuchinskas, H. Youn, R.L. Kerby, G.P. Roberts, T.L. Poulos, T.G. Spiro, *J. Inorg. Biochem.* **101**, 1776 (2007)
44. B. Chazallon, Y. Celik, C. Focsa, Y. Guinet, *Vib. Spectrosc.* **42**, 206 (2006)
45. R.J. LeBlanc, C.T. Williams, *J. Mol. Catal. A* **220**, 207 (2004)

46. S.W. Lee, Y.-B. Shin, K.S. Jeon, S.M. Jin, Y.D. Suh, S. Kim, J.J. Lee, M.-G. Kim, *Ultramicroscopy* **108**, 1302 (2008)
47. M.L. Calegari, H.B. Suffredini, S.A.S. Machado, L.A. Avaca, J. Power Sources **156**, 300 (2006)
48. G. Socrates, *Infrared and Raman characteristic group frequencies: tables and charts*, 3rd edn. (Wiley, West Sussex, 2004), p. 122
49. M.J. Giz, G.A. Camara, J. Electroanal. Chem. **625**, 117 (2009)
50. M.J.S. Farias, G.A. Camara, A.A. Tanaka, T. Iwasita, J. Electroanal. Chem. **600**, 236 (2007)
51. F.H.B. Lima, E.R. Gonzalez, *Electrochim. Acta* **53**, 2963 (2008)
52. F. Vigier, C. Coutanceau, F. Hahn, E.M. Belgsir, C. Lamy, J. Electroanal. Chem. **563**, 81 (2004)
53. X.H. Xia, H.D. Liess, T. Iwasita, J. Electroanal. Chem. **437**, 233 (1997)
54. G.A. Camara, T. Iwasita, J. Electroanal. Chem. **578**, 315 (2005)
55. A. Bruckbauer, A. Otto, *Surf. Sci.* **502–503**, 394 (2002)
56. I. Mrozek, C. Pettenkofer, A. Otto, *Surf. Sci.* **238**, 192 (1990)